Scattering of Low Energy Atoms by Surfaces: The Helium–Copper Systems

G. ARMAND, J. LAPUJOULADE, J. R. MANSON,*
J. PERREAU AND B. SALANON
Service de Physique des Atomes et des Surfaces,
Centre d'Etudes Nucléaires de Saclay, 91191 Gif-sur-Yvette Cedex, France

(*Received 23 August 1982*)

Abstract. A number of experimental results for the diffraction of low energy helium by closely packed and stepped copper surfaces is presented. Observation of selective adsorption resonances shows that the surface average of the interaction potential is the same for all crystal faces. The thermal attenuation of the scattered intensities is given by a modified Debye–Waller factor. These results are interpreted in terms of interaction potentials with a soft exponential repulsion and an attractive well using an exact method based on Neumann iteration of the transition matrix equation. Good agreement with experiment is obtained in several systems over a large range of scattering energies.

I. INTRODUCTION

The scattering of light, low energy atoms and molecules has long been recognized as having an excellent potential for giving a great deal of information about surfaces and the interactions that can occur at surfaces.[1] In this paper we would like to present a number of experimental results for the scattering of helium by a variety of closely packed and stepped Cu surfaces and also to develop the theoretical methods that have been used to interpret these data.

Light atoms and molecules are particularly suitable as surface probes since at low energies they neither penetrate nor distort appreciably the crystal structure and hence only the outer layer is sampled. At thermal energies the de Broglie wavelength is comparable to the lattice spacing, thus by observing surface diffraction one can determine the surface structure.[2,3] For similar reasons low energy atoms should be good projectiles for investigating inelastic processes,[4] particularly those involving Rayleigh or surface phonons.[5]

Figure 1 gives a typical example of the diffraction pattern observed for a monoenergetic helium beam scattered by the Cu (115) stepped surface.[6,7] The beam is incident at an angle of 28° with respect to the surface normal and at an energy of 63 meV ($k_i = 11$ Å^{-1}, $\lambda_i = 0.57$ Å). The beam is perpendicular to the stepped rows and incident in the "upstairs" direction as indicated by the arrows in Fig. 2. Figure 1 shows the peaks diffracted in the plane of incidence. Peaks scattered out of the plane of incidence were not measurable with the experimental apparatus, but they are believed to be small. In fact, experiments on the (110) surface with the incident beam parallel to the widely spaced rows failed to reveal any diffracted peaks, consistent with the fact that the surface is close packed in this direction and shows a negligible corrugation. Considerably more than ten peaks are clearly observed in Fig. 1 with many of the diffracted peaks even larger than the specular beam, demonstrating that this type of experiment can be explained only by a strong scattering theory.

The interaction potential between the incoming particle and a surface basically may be separated into three

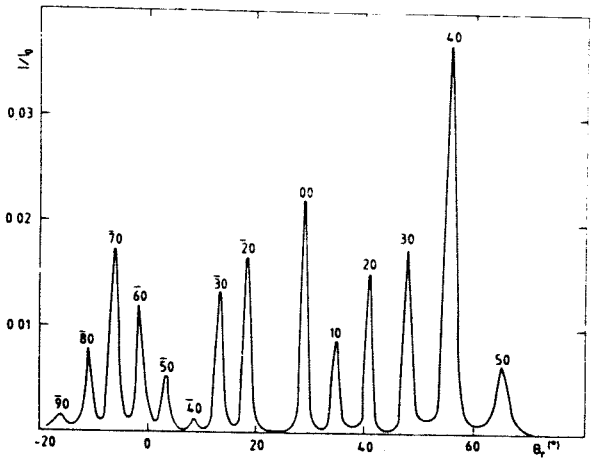

Fig. 1. The in-plane diffraction intensities as a function of azimuthal scattering angle θ_f for a 63 meV He beam incident with $\theta_i = 28°$ on a Cu (115) surface. The step rows are perpendicular to the plane of incidence.

regions: the long range attractive van der Waals force, the repulsive force at the surface and, in between, an attractive well containing the bound physisorption states. Since the two-body van der Waals force follows a $1/r^6$ power law, by simple argument, for the atom–surface system, it may be represented as C_3/z^3, where z is the perpendicular distance from the surface.

The repulsive force is primarily a result of the Pauli exclusion between electrons of the incoming particle and those of the surface. Recent calculations indicate that the repulsive force is approximately proportional to the electron density at the surface[8] and is thus expected to be very closely exponential in form. Further calculations seem to show that observations of the surface corrugations by diffraction experiments may provide a great deal of information on the surface electron density.[9]

* Permanent address: Department of Physics and Astronomy, Clemson University, Clemson, SC 29631 USA.

The effect of the bound states can be very important in a scattering experiment since they give rise to resonant behavior. Such resonance occurs whenever the incident beam can diffract into a bound state while still conserving total energy, i.e. the total energy is always positive corresponding to the atom constrained to move parallel to the surface with a speed higher than the incident speed. Since the total energy is positive the particle must eventually leave the surface by a similar mechanism but these resonances can sharply alter the distribution of intensities in the diffracted peaks. Figure 3 shows a plot of the specular intensity as a function of incident angle for the He/Cu (115) system at an incident energy of 21 meV. The resonances are manifest as sharp maxima or minima with relatively narrow linewidths. Since the positions of the resonances give with high accuracy the bound state levels, the form of the attractive region of the potential as well as the van der Waals constant C_3 can be determined quite readily.

It is clear, a priori, that atom scattering experiments in principle provide virtually all information that one can gain about the surface interaction. The object of this brief introduction is to demonstrate a particularly nice aspect of such experiments, that different types of experiments can give detailed information about specific different components of the potential.

In this paper we discuss primarily elastic scattering, but there is one aspect of inelastic scattering that must be taken into account and this is the thermal attenuation of the diffracted beams caused by the surface vibrations. As in the case of bulk X-ray or neutron scattering the thermal attenuation can be accounted for by a Debye-Waller factor, a decreasing exponential whose argument is proportional to both the temperature (or, more precisely, the mean-square surface displacement) and the square of the momentum transfer. At the moment, a Debye-Waller type behavior can be justified on theoretical grounds only for certain very special models, notably those in which the collision time is very short, such as for a hard-wall model.[10,11] However, for the case of a He–metal collision, a Debye-Waller type of thermal attenuation is an experimental reality, as is seen from the typical example given in Fig. 4. The logarithms of the peak intensities as a function of surface temperature from 77 to 750 °K for a 63 meV beam incident on Cu (110) at an angle of 50.5° are shown. These decrease linearly with temperature, as expected, over a large range while at high temperatures anharmonic effects seem to be important. (The high temperature deviation of the very weak $(\bar{2}0)$ peak is probably an experimental artifact, due to inelastic background effects.) The experimental intensities to be compared with those obtained using the elastic theory are the extrapolations of the intensities to 0 °K.[6,12] When this extrapolation is combined with a correction in higher orders of temperature to account for anharmonicity, a very consistent picture of the surface mean-square displacement emerges.[13]

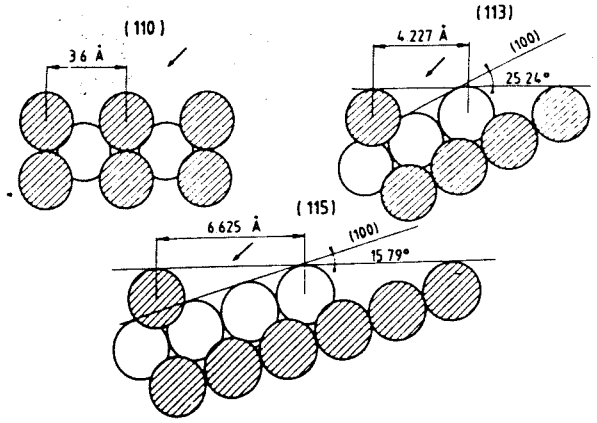

Fig. 2. The crystal structure of the (110), (113) and (115) surfaces of Cu. The arrow indicates the direction of the incident He beam for the experiments reported here.

II. THEORY

A model which has been extremely useful in interpreting the scattering data is to represent the repulsive part of the potential by an inpenetrable wall with corrugations

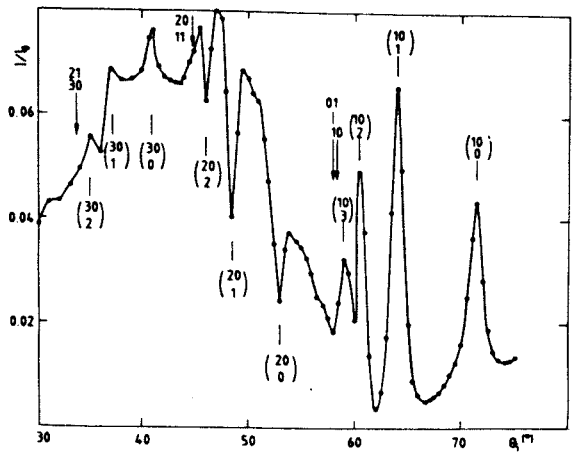

Fig. 3. The specular intensity as a function of incidence angle for a 21 meV He beam on a Cu (113) surface. The lines denote the kinematical position of the resonances and are labeled by the associated reciprocal lattice vector and bound state. The arrows indicate the thresholds at which an evanescent state becomes a diffracted beam.

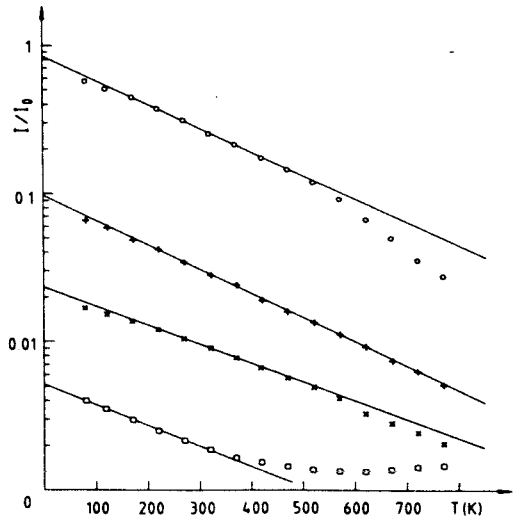

Fig. 4. A typical Debye-Waller plot of the logarithm of diffracted beam intensities as a function of crystal temperature. A 63 meV He beam is incident on a Cu (110) surface at an angle of 32.5°. The experimental data are as follows: ○ — specular or (00) peak; + — $(\bar{1}0)$ peak; × — (10) peak; and □ — $(\bar{2}0)$ peak.

reflecting the periodicity of the surface atoms. This corrugated hard wall model (CHW) can be represented by the potential

$$V(r) = \begin{cases} \infty; & z < \varphi(R) \\ V(R,z); & z > \varphi(R) \end{cases} \quad (1)$$

where z, as above, is the direction perpendicular to the surface, and R is a vector lying in the surface. The function $\varphi(R)$ gives the corrugation of the wall and $V(R,z)$ (which is usually taken to be independent of R) is chosen to have the correct asymptotic behavior and bound state energies which agree with observed resonance behavior. An exact solution to (1) is by no means simple even when $V(R,z)$ is a constant.[14-16] However, the problem is amenable to a variety of approximations which are particularly applicable to surfaces which are not too strongly corrugated.[17] The model in Eq. (1) has been reasonably successful in explaining the scattering of He from alkali halide surfaces[18,19] but, as we point out in Section III below, a rigid wall model is inadequate for explaining the scattering from metal surfaces where a small penetration of the wavefunction into the surface is important.

In order to have particle penetration the surface must be made non-rigid or "soft" and this can be done in two distinct ways. The first possibility is to consider a finite step, for example by replacing $V(r) = \infty$ by $V(r) = V_0$ for $z < \varphi(R)$ in Eq. (1). This type of potential has a particle penetration which increases with increasing incident energy, the penetration depth being essentially $\sqrt{2m(V_0 - E_i)}/\hbar$ where E_i is the incident energy. On the other hand, an exponential repulsive potential, $V(r) \propto \exp[-2\kappa z]$ (suggested by considerations of the form of the electron density near the surface), gives a wave penetration which is larger for low incident energies than for high energies. Calculations for a step potential with corrugations do not give results that are appreciably different from the CHW[20] and, as demonstrated by the comparison with experiment in Section III, it is the exponential form which is correct.

A soft wall potential can always be expanded in a Fourier series

$$V(r) = v_0(z) + \sum_{G \neq 0} V_G(z) e^{iG \cdot R} \quad (2)$$

where G is a surface reciprocal lattice vector and $v_0(z)$ is the surface average of $V(r)$. A variety of approaches have been put forward for obtaining the scattered intensities by starting from Eq. (2) and directly integrating Schrödinger's equation by the method of close coupling. These methods are, in principle, exact solutions but have the disadvantage that for all but the weakly corrugated surfaces they require a large amount of computer time.[21]

The methods that we would like to discuss here are based on the transition matrix equation in the two-potential formalism. The potential is written, as suggested in Eq. (2), as the sum of two parts, $V(r) = U + v$, where U is a strong part which backscatters all incident particles (we note in passing, however, that $U = v_0(z)$ is not always the most appropriate choice). Then the scattered intensities are readily obtained from the distorted wave transition matrix obeying the equation:

$$t_{fi} = v_{fi} + \sum_p v_{fp}(E_i - E_p + i\varepsilon)^{-1} t_{pi} \quad (3)$$

where the v_{pq} are matrix elements of v taken with respect to eigenstates of U. Generally, in obtaining Eq. (3) one has to be careful in defining the difference between outgoing and incoming solutions to $V(r)$ and U. However, in surface scattering such questions are trivial; the difference between an outgoing and an incoming solution of U is simply a phase factor equivalent to the S-matrix for specular scattering.

An example of one of the potentials to which this formalism has been applied is the corrugated Morse potential defined by

$$V(r) = D\{\exp[2\kappa(\varphi(R) - z)]/v_0 - 2\exp[-\kappa z]\} \quad (4)$$

where v_0 is the surface average of $\exp[2\kappa\varphi(R)]$. If this is expanded as in Eq. (2), $v_0(z)$ is given by a Morse potential and the higher-order Fourier components are

$$v_{G\neq 0}(z) = De^{-\kappa z} v_G / v_0 \quad (5)$$

with

$$v_G = \frac{1}{S}\int_{uc} dR e^{-iG\cdot R} e^{+2\kappa\varphi(R)} \quad (6)$$

where S is the area of the unit cell (uc).

Then the diffracted intensities can be written in terms of a dimensionless transition matrix $F_G(q)$ as

$$I_G = |\delta_{G,0} - i\pi F_G(p_G)/4\sqrt{p_0 p_G}|^2 \quad (7)$$

where p_G is the dimensionless perpendicular wave vector associated with the Gth diffracted beam

$$p_G = k_{Gz}/\kappa = \sqrt{k_0^2 - (K_0 + G)^2}/\kappa \quad (8)$$

and k_0 is the incident wave vector with components K_0 and k_{0z} parallel and perpendicular to the surface, respectively.

Equation (3) becomes the following set of coupled equations for the $F_G(p)$ functions:

$$\begin{aligned} F_J(r) = {} & \lambda_{J,0} f(r,p_0) - \frac{1}{4}\sum_N \lambda_{J,N}\int_0^\infty dq f(r,q) F_N(q) \\ & \times [q^2 - p_N^2 + i\varepsilon]^{-1} \\ & + \frac{1}{4\pi^2}\sum_N \lambda_{J,N}\sum_n l(r,n) F_N(n) \\ & \times [p_N^2 + d^2 - 2d(n+\tfrac{1}{2}) + (n+\tfrac{1}{2})^2]^{-1}, \end{aligned} \quad (9)$$

$$\begin{aligned} F_J(n) = {} & \lambda_{J,0} l(p_0,n) - \frac{1}{4}\sum_N \lambda_{J,N}\int_0^\infty dq l(q,n) F_N(q) \\ & \times [q^2 - p_N^2 + i\varepsilon]^{-1} \\ & + \frac{1}{4}\sum_N \lambda_{J,N}\sum_m M(n,m) F_N(m) \\ & \times [p_N^2 + d^2 - 2d(m+\tfrac{1}{2}) + (m+\tfrac{1}{2})^2]^{-1}, \end{aligned} \quad (10)$$

where n is an integer denoting the band states, $d^2 = 2mD/\hbar^2\kappa^2$, and $\lambda_{J,N} = (1 - \delta_{J,N})v_{J-N}/v_0$. The matrix elements of $\exp[-2\kappa z]$ with respect to Morse potential eigenfunctions are written as $f(p,q)$, $l(p,n)$ and $M(n,m)$ for continuum–continuum, continuum–bound, and bound–bound transitions, respectively.

There are a number of methods that have been used to resolve Eqs. (9) and (10). One can discretize the integrals and then invert the resulting matrix equation. This has been done for the case of a purely repulsive corrugated exponential potential (i.e., the repulsive term of Eq. (4)) but for all except very weakly corrugated surfaces the

procedure requires too much computer memory space.[22] The integral can also be reduced to discrete matrix form by expanding $F_j(r)$ in a complete set of states, such as Laguerre polynomials. Again, even for the simpler corrugated exponential potential this leads to inordinate demands on the computer memory.

A method which has proven to be very successful is to solve these coupled integral equations by Neumann iteration until they converge, a process completely equivalent to distorted wave pertubration theory carried out to high order.[23] This has been applied to the exponential corrugated potential, the corrugated Morse of Eq. (4) and a modified Morse-type potential described in Section III below. This iteration method converges over a large domain of variously corrugated surfaces. The exponential corrugated potential, for which the convergence properties have been most closely checked, gives good solutions for virtually all surfaces of current interest, including the alkali halides such as LiF.[24] However, to obtain convergence for high corrugation amplitudes one must choose U not as the surface average of $V(r)$, but displaced with respect to the surface average, or even with a different well depth D as in the case of the Morse potential.

When combined with the appropriate projection techniques, as discussed in Section IV below, the iteration method converges equally well with or without conditions for resonances with bound states.

III. COMPARISON WITH EXPERIMENTAL RESULTS

Detailed measurements of the He diffraction intensities from a variety of closely packed and stepped Cu surfaces have been carried out.[6,7] In this section we will narrow the discussion to a consideration of the (110) and (113) surfaces, for which we have the most detailed comparisons with theory. These comparisons clearly show that a hard-wall model of the repulsive potential fails to explain the data but an exponential repulsion gives quite good agreement. Figure 5 shows the diffraction intensities for a 63 meV He beam incident on Cu (110) as a function of incidence angle θ_i, together with results of four different theoretical models.

The experimental data shown with error bars are obtained by extrapolation to zero temperature and renormalizing the sum of in-plane diffraction intensities to unity. The renormalization is carried out in order to eliminate the effects of possible out-of-plane diffraction in comparison with the one-dimensional calculations. The four theoretical models correspond to the corrugated Morse potential of Eq. (4), the corrugated exponential potential, the corrugated hard wall, and the corrugated hard wall with an attractive well, all with the same one-dimensional sinusoidal corrugation:

$$\varphi(x) = ha\cos(2\pi x/a), \tag{11}$$

with $a = 3.6$ Å.

The well depth for the Morse and hard wall models was taken as 6.35 meV, the value given by examination of the resonance behavior as discussed in Section IV below. The value of $\kappa = 1.05$ Å^{-1} for the range parameters in the Morse potential gives the best fit for all surfaces and all energies considered. It is clear from Fig. 5 that the corrugated Morse potential gives a good fit to the experiment, far better than either of the hard wall models. In fact, the only way a hard wall model can be made to fit the data is to choose a different corrugation for each incident angle.

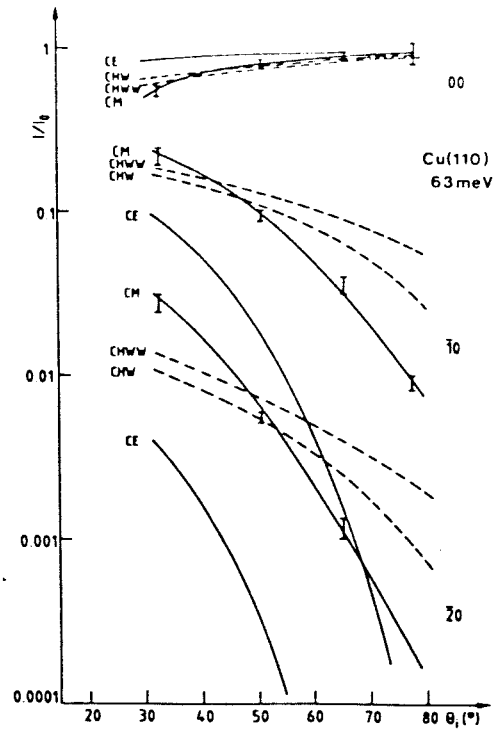

Fig. 5. Comparison between the experimental data and four theoretical models for the scattering of 63 meV He by a Cu (110) surface: CHW, corrugated hard wall with corrugation parameter $h = 0.013$; CHWW, corrugated hard wall with well, $h = 0.013$ and well depth 6.35 meV; CE, corrugated exponential, $h = 0.012$, $\kappa = 1.05$ Å^{-1}; CM, corrugated Morse potential, $h = 0.012$, $\kappa = 1.05$ Å^{-1} and $D = 6.35$ meV. The incident plane is perpendicular to the closely packed rows.

Equally good agreement is found for the same experiment as in Fig. 5 but with an incident energy of 21 meV. The only adjustment that must be made is to decrease the corrugation parameter h from 0.012 to a value of 0.008 in the Morse potential calculation. This decrease in corrugation with incident energy is in agreement with recent theoretical predictions indicating that the corrugation is given directly by the electron density.[8,9]

Figure 6 shows the comparison of the experiment with the corrugated Morse potential for a 21 meV He beam scattered by the Cu (113) surface. The non-renormalized data are shown and the calculation is for the two-dimensional unit cell in the form of a parallelogram having the corrugation function

$$\begin{aligned}\varphi(x,y) = a\Big\{ & h_{10}\cos\frac{2\pi x}{a} + h_{01}\cos\left(\frac{\pi x}{a}\right)\cos\left(\frac{2\pi y}{b}\right) \\ & + h_{11}\cos\left(\frac{3\pi x}{a}\right)\cos\left(\frac{2\pi y}{a}\right) \\ & - c_{01}\sin\left(\frac{\pi x}{a}\right)\cos\left(\frac{2\pi y}{b}\right)\Big\}\end{aligned} \tag{12}$$

with $b = 2.55$ Å, the nearest neighbor distance, and $a = 4.227$ Å, the distance between steps. The corrugation parameters are $h_{10} = 0.017$, $h_{01} = 0.01$, and $h_{11} = C_{01} = 0$. The agreement between theory and experiment is reasonably good over a large range of incident angles. In contrast, similar calculations for a hard wall model give very poor agreement, as was found for the 110 surface of Fig. 5.

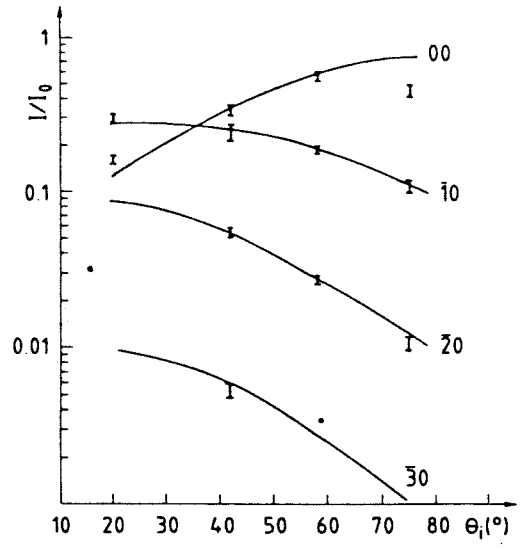

Fig. 6. Comparison between experiment and the results of the corrugated Morse potential with the two-dimensional corrugation of Eq. (12) for a 21 meV He beam incident on Cu (113).

For the same system as illustrated in Fig. 6, equally good agreement is obtained at the higher energy of 63 meV. The only change that must be made is to augment the principal corrugation parameter h_{10} by approximately 25%. Although the increase in corrugation strength with incident energy is in agreement with theoretical predictions, it points out the inadequacy of the corrugated Morse potential model in representing correctly the corrugation at all energies without changing parameters. In fact an examination of the corrugated Morse potential shows that the effective corrugation at fixed energy actually decreases with energy, a trend opposite to the desired behavior.

In order to improve this situation we have considered a modification of the corrugated Morse potential which shows a natural increase in effective corrugation with energy. Simply stated, in the Fourier components of Eq. (5) we change the strength D to γD and adjust the range parameters from κ to κ', while leaving the zero order term (the surface average of $V(r)$) the same Morse potential. This potential can be written in closed form as

$$V(z,\boldsymbol{R}) = D\{\gamma(\exp[2\kappa\varphi(\boldsymbol{R})]/v_0 - 1)Z^{2\kappa'/\kappa} + Z^2 - 2Z\}, \tag{13}$$

with

$$Z = \exp[-\kappa z]. \tag{14}$$

In order to obtain an increase of the effective corrugation amplitude with energy, κ' must be taken greater than κ. For the He/Cu (110) system discussed below a value of $2\kappa'/\kappa = 3$ was the appropriate choice, which is also favorable for the analytical calculation of the matrix elements.

Measurements of the diffraction intensities for the He/Cu (110) system have been made over a range of energies from 21 to 240 meV. Good agreement can be obtained with the corrugated Morse potential by adjusting the corrugation parameter h for each energy. However, using the Modified Corrugated Morse Potential from Eq. (13) with $h = 0.169$ and $\gamma = 0.0235$ gives excellent agreement for all energies without further changes in the parameters. An example for an incident energy of 125 meV is given in Fig. 7. Thus, with the modified Corrugated Morse Potential of Eq. (13), we have a model of the He–Cu interaction that is capable of reproducing the experimental intensities over an energy range of an order of magnitude and at all incident angles measured.

IV. RESONANCES

Clear resonance behavior was observed on the stepped Cu surfaces, as shown in Fig. 3, but not on the more closely packed (110) surface. By comparing the positions of the resonance peaks to the kinematical conditions for a resonance, i.e. conservation of energy and parallel momentum,

$$E_0 = \frac{\hbar^2}{2m}(k_{0z}^2 + K_0^2) = \frac{\hbar^2}{2m}(\boldsymbol{K}_0 + \boldsymbol{G})^2 - \varepsilon_n. \tag{15}$$

The bound state energies ε_n were determined. These energies are 4.45 ± 0.15, 2.1 ± 0.1, 0.90 ± 0.1 and 0.35 ± 0.15 meV, which are reproduced by a Lennard-Jones 9-3 potential

$$V(z) = (3^{3/2}/2)D\{(\sigma/z)^9 - (\sigma/z)^3\} \tag{16}$$

with $\sigma = 2.7 \pm 0.1$ Å and $D = 6.35 \pm 0.05$ meV.

A very interesting point is that although the resonance strength and linewidths depend on the surface corrugation, the energy levels are the same for the (113) and (115) surface and are consistent with previous measurements of the (117) face. (The fact that resonances were not observed on the (110) face is consistent with calculations discussed below, which show that the linewidths are too narrow to be observed.) The fact that the energy levels are the same for all faces demonstrates that the division of the potential into a surface average plus higher-order Fourier components as in Eq. (2) is a reasonable and valid assumption, and it implies that the attractive part of the surface potential is a collective effect not strongly influenced by the corrugation of the outermost layer.

The theoretical problem posed by the resonances is that they represent divergences in the transition matrix

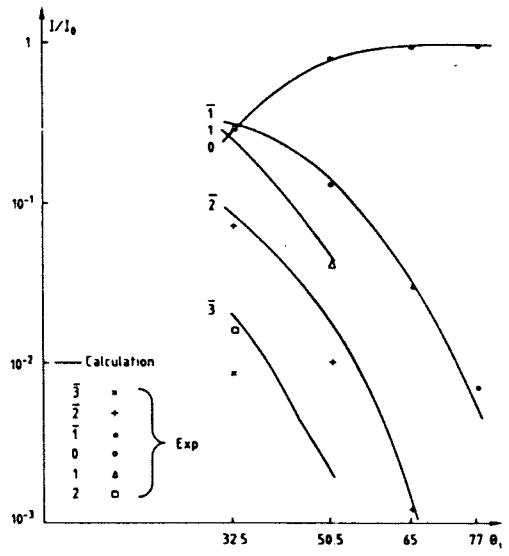

Fig. 7. The diffracted intensities as a function of incident angle for 125 meV He scattered by Cu (110) compared with the calculations for the modified Corrugated Morse potential of Eq. (13).

equation. This can be seen in Eqs. (9) and (10), where the resonance condition (15) is identical with the vanishing of one of the denominators in the bound state sums, thus a method based on iteration will not converge. These divergences can be circumvented by simple projection techniques similar to those developed in nuclear physics.[18,25] Formally, the transition operator obeys the relation $t = v + vGt$. We can write $G = G_1 + G_2$ and then it is readily shown that the transition operator is given by the pair of equations

$$t = h + hG_1t$$

and

$$h = v + vG_2h,$$

or in matrix element form

$$t_{fi} = h_{fi} + \sum_b{}' h_{fb}(E_i - E_b)^{-1}t_{bi}, \tag{17}$$

$$h_{fi} = v_{fi} + \sum_l v_{fl}(E_i - E_l + i\varepsilon)^{-1}h_{li}. \tag{18}$$

If we place all resonant terms in G_1 then the singular denominators do not appear in the sum in Eq. (18) for the h_{fi}, thus the h-matrix is still amenable to an iteration solution. The t-matrix is subsequently obtained from Eq. (17) by inversion of a small matrix involving only the resonant bound states.

As a specific example, for a simple resonance involving only a single bound state b the transition matrix is of the form

$$t_{fi} = h_{fi} + h_{fb}h_{bi}/(E_i - E_b - h_{bb}). \tag{19}$$

It is clear from the presence of the term h_{bb} in the denominator, that the resonance associated with the kinematical condition $E_i = E_b$ no longer gives rise to a divergence, but is shifted in energy by $\mathrm{Re}\,h_{bb}$ and has a linewidth determined by $\mathrm{Im}\,h_{bb}$. If the appropriate dimensionless form of Eq. (18) is inserted for the diffracted beam intensity in Eq. (7) we obtain the standard form

$$I_G = A^2|1 - ib/(x - i)|^2, \tag{20}$$

where the explicit values of A, b and x are obvious. By examination of this form the signatures of the resonances can be characterized as a function of incident energy E_i or incident angle θ_i.[26,27] In general, if b is complex the resonance as a function of E_i or θ_i will have two extrema, a minimum and a maximum. If b is real, or nearly so, one of the extrema disappears and the resonance is of Lorentzian form, a minimum if $-2 < b < 0$ and a maximum otherwise. An important advantage of this projection method is that generally in Eq. (20) A and b are slowly varying and only the variation in the normalized energy difference x is important. Then, to a very good approximation, the whole resonance can be mapped out by calculating A and b at a single point near the resonance and then considering I_G to be a function of x alone. In the case of multiple or simultaneous resonances the entire resonance region can be mapped out in a very similar manner.

The resonance calculations carried out with the corrugated Morse potential for the Cu (110) surface corresponding to the experimental observation conditions give, in the specular beam, for instance, maxima with a very narrow angular width of approximately 0.02°. Even with substantial broadening due to inelastic effects, such resonances are not observable within the experimental angular resolution of 0.2–0.5° which, as mentioned above, explains why they were not observed on the Cu (110) face.

Calculations for the resonances observed on the (113) surface using the one-dimensional corrugation function of Eq. (14) give rather narrow maxima in the specular beam rather than the minima observed in the experiment. This is because the resonant state only couples strongly with the specular beam. This corresponds to Eq. (19) with $-b \gtrsim 2$.[26,27] The magnitude of $\mathrm{Re}\,b$ can be reduced by adding additional diffraction channels out-of-plane that couple with the resonance. The fact that the sum of the zero-temperature extrapolated diffraction intensities is slightly less than unity indicates that there may be some small out-of-plane peaks, which is why the calculations in Fig. 6 were done with the two-dimensional corrugation of Eq. (12).

Shown in Fig. 8 is a typical calculation, in this case for the resonance of the (10) reciprocal lattice with the lowest ($n = 0$) bound state at an energy of 21 meV. The corrugation is given by Eq. (12), with $h_{10} = 0.017$, $h_{01} = -h_{11} = 0.006$ and $C_{01} = -0.002$. The effect of the out-of-plane diffraction is to reduce the magnitude of $\mathrm{Re}\,b$ but enhance $\mathrm{Im}\,b$ producing the double structure with a slightly predominant minimum. If inelastic events were included in the calculation more channels would be coupled to the resonance, and it is virtually certain that the structure would have a pronounced minimum in better agreement with experiment, as has been demonstrated with hard-wall models for the scattering of He by graphite.[28–30] In general, we can say that for a calculation of diffraction intensities a one-dimensional corrugation is usually sufficient for these stepped surfaces except close to resonance conditions, where small out-of-plane scattering may have a large effect and inelastic events seem to be quite imporant.

V. CONCLUSIONS

This paper is a brief review of some of the progress that has been made at Saclay in the domain of low-energy atom surface scattering from metal surfaces. A theory has been developed for obtaining the elastic scattering intensities for soft wall potential models based

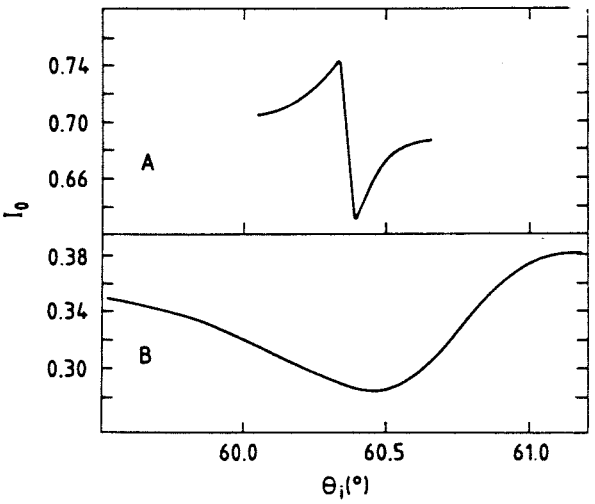

Fig. 8. Behavior of the specular peak as a function of the incidence angle in the region of resonance of the (10) reciprocal lattice vector with $n = 0$ bound state for He/Cu (113) at an energy of 21 meV. A. Calculation using the Morse potential with $\kappa = 1.05$ Å^{-1}, $D = 6.35$ meV, and the corrugation function from Eq. (12). B. Experimental curve.

on Neumann iteration of the complete transition matrix equations. The method is exact, and for several potentials to which it has been applied converges over a large range of different surface corrugations. With appropriate projection techniques the method converges equally rapidly in and out of resonance conditions.

The experimental results presented here are drawn from a large number of measurements of diffraction intensities from a variety of closely packed and stepped Cu surfaces. Observations of the resonance phenomena are consistent with all surfaces of copper studied having the same bound state energy levels. This implies that the assumption of writing the interaction potential as a sum of Fourier components in the lattice periodicity is not only good, but that the zero component (the surface average) is the same for all faces, and only the higher components change, i.e. those terms giving the corrugation.

Calculations of the diffraction intensities close to resonance conditions, using the iteration method with the Morse potential, are not completely successful and it appears that a proper inclusion of inelastic effects will be necessary in order to obtain good agreement with the forms of the resonances. However, it is clearly demonstrated that the effects of small out-of-plane diffraction peaks can be very important under resonance conditions.

An excellent interpretation of the diffraction intensities as a function of the incidence angle was obtained using the corrugated Morse potential model for all faces calculated and for energies from 21 to 240 meV. The corrugation amplitude was observed to increase monotonically with incident energy. On the other hand, the currently popular corrugated hard wall model with an attractive well is shown to be totally inadequate to explain the data, implying that soft wall effects are important in atom surface scattering.

Furthermore, a modified corrugated Morse potential is presented which naturally includes the increase of surface corruation with energy. This model is shown to be capable of reproducing the experimental data for the He/Cu (110) system over the entire range of energies (21–240 meV) with the same parameters. Both the experimental behavior of the repulsive part of the potential and the increase in effective corrugation of the potential with incoming energy are in accord with recent observations that the interaction potential should be proportional to the surface electronic density. The agreement between experiment and theory observed here represents a clear demonstration that the interaction potential has essentially the same form as the electron density, and it also points out the ability of atom and molecule scattering experiments to obtain such information about the surface.

REFERENCES AND NOTES

1. For recent review articles see H. Hoinkes, *Rev. Mod. Phys.*, **52**, 993 (1980); G. Armand and J. Lapujoulade in R. Campargue, ed., *Proceedings of the 11th International Symposium on Rarefied Gas Dynamics*, C.E.A., Paris, 1979, p. 1329; F. O. Goodman, *Prog. Astronaut. Aeronaut.* **74**, 3 (1981); V. Celli, ibid., 50.
2. J. E. Lennard-Jones and A. F. Devonshire, *Proc. R. Soc. London, Ser. A*, **158**, 253 (1937).
3. N. Cabrera, V. Celli, F. O. Goodman and R. Manson, *Surf. Sci.*, **19**, 67 (1970).
4. A. F. Devonshire, *Proc. R. Soc. London, Ser. A*, **158**, 269 (1937); C. Strachan, *Proc. R. Soc. London Ser. A*, **150**, 456 (1935).
5. N. Cabrera, V. Celli and R. Manson, *Phys. Rev. Lett.*, **32**, 346 (1969).
6. J. Perreau, Thèse de Troisième Cycle, Université de Paris, unpublished.
7. For details of the experimental apparatus see Ref. 6 or Ref. 12.
8. N. Esbjerg and J. K. Nørskov, *Phys. Rev. Lett.*, **45**, 807 (1980).
9. D. R. Hamman, *Phys. Rev. Lett.*, **46**, 1227 (1981).
10. G. Armand and J. R. Manson, *Surf. Sci.*, **80**, 532 (1979).
11. A. C. Levi and H. Suhl, *Surf. Sci.*, **88**, 221 (1979).
12. J. Lapujoulade, Y. Lejay and N. Papanicolaou, *Surf. Sci.*, **90**, 133 (1979).
13. Lapujoulade, J. Perreau and A. Kara, to be published.
14. N. Garcia and N. Cabrera in R. Dobrozemsky et al., eds., *Proceedings of the Seventh International Vacuum Congress and the Third International Conference on Solid Surfaces, Vienna*, Berger, Vienna, 1977, p. 379.
15. G. Armand and J. R. Manson, *Phys. Rev. B*, **18**, 6510 (1978).
16. B. Salanon and G. Armand, *Surf. Sci.*, **112**, 78 (1981).
17. N. Garcia, *J. Chem. Phys.*, **67**, 897 (1977); C. Lopez, F. Yndurain and N. Garcia, *Phys. Rev. B*, **18**, 970 (1978).
18. C. E. Harvie and J. H. Weare, *Phys. Rev. Lett.*, **40**, 187 (1978).
19. N. Garcia, F. O. Goodman, V. Celli and N. R. Hill, *Phys. Rev. B*, **19**, 1808 (1979).
20. J. R. Manson and G. Armand, *Phys. Rev. B*, **20**, 5020 (1979).
21. G. Wolken, *J. Chem. Phys.*, **58**, 3047 (1973); *J. Chem. Phys.*, **61**, 456 (1974); A. Leibsch and J. Harris, *Surf. Sci.*, **L111**, 721 (1981); R. B. Laughlin, *Phys. Rev. B*, **25**, 2222 (1982); A. Tsuchida, *Surf. Sci.*, **46**, 611 (1974).
22. G. Armand and J. R. Manson, *Phys. Rev. Lett.*, **43**, 1839 (1979).
23. G. Armand, *J. Phys. Paris*, **41**, 1475 (1980).
24. G. Armand and J. R. Manson, *Phys. Rev. B*, **25**, 6195 (1982).
25. H. Feshbach, *Ann. Phys. NY*, **5**, 537 (1958).
26. K. Wolfe and J. Weare, *Phys. Rev. Lett.*, **41**, 1663 (1978).
27. V. Celli, N. Garcia and J. Hutchison, *Surf. Sci.*, **87**, 112 (1979).
28. J. S. Hutchison, *Phys. Rev. B*, **22**, 5671 (1980).
29. N. Garcia, W. Carlos, M. Cole and V. Celli, *Phys. Rev. B*, **21**, 1936 (1980).
30. Karen L. Wolfe and John H. Weare, *Surf. Sci.*, **94**, 581 (1980).